



INTEGRAL

Announcement of Opportunity for Observing Proposals (AO-2)

OMC Observer's Manual

Written by: Astrid Orr
Integral Science Operations, ESTEC

based upon inputs from:
M. Mas Hesse, OMC PI, LAEFF/INTA, Madrid

15 July 2003
Issue 2

Ref. nr. INT-SOC-DOC-024

This page was intentionally left blank

Table of Contents

I.	Introduction	5
II.	Description of the instrument	7
1.	Overall design	7
2.	The optics	7
3.	The CCD detector	7
III.	Instrument operations	10
1.	Normal science operations mode	10
2.	Fast monitoring mode	11
3.	The OMC input catalogue.	11
4.	Gamma-ray bursts and transient sources	12
IV.	Instrument performances	13
1.	Background and read-out noise	13
2.	Limiting faint magnitude	13
3.	Limiting bright magnitude	17
4.	Photometric accuracy	17
5.	Focusing	20
V.	Data products	21

This page was intentionally left blank

I. Introduction

The Optical Monitoring Camera (OMC) is a wide-field optical instrument using a large-format CCD detector, limited by a relatively low telemetry rate. It measures the optical emission from the prime targets of the two gamma-ray instruments SPI and IBIS. The OMC offers the first opportunity to make observations of long duration in the optical band simultaneously with those at hard X-rays and gamma-rays. Multi-band observations are particularly important in high-energy astrophysics where variability is typically rapid, unpredictable and of large amplitude. The main objectives of the Optical Monitoring Camera can be summarised as follows:

- a) To monitor during extended periods of time the optical emission of all high-energy targets within its field of view, simultaneously with the high-energy instruments.
- b) To provide simultaneous and calibrated standard V-band photometry of the high-energy sources to allow comparison of their high-energy behavior with previous or future ground-based optical measurements.
- c) To analyse and locate the optical counterparts of high-energy transients detected by the other instruments, especially gamma-ray transients.
- d) To monitor any other optically variable sources serendipitously within the OMC field of view, which may require long periods of continuous observations for their physical understanding (variable stars, flaring and eruptive objects, etc.).

The purpose of this manual is to present all the information about the OMC which is necessary for the preparation of Integral proposals.

Table 1: OMC parameters and scientific performances

Parameter	In-orbit value
Field of view	$4.979^\circ \times 4.979^\circ$
Aperture	5 cm diameter
Focal length	153.7 mm (f/3.1)
Optical throughput	> 70% at 550 nm
Stray light reduction factor ^a (within UFOV ^b)	$\ll 10^{-4}$ (no stray light detected)
Angular resolution	$\approx 25''$ Gaussian PSF (FWHM \approx 1.4 pixels)
Point source location accuracy	$\approx 6''$
Angular pixel size	$17.504'' \times 17.504''$
CCD pixels	2055×1056 (1024×1024 image area) ($13 \times 13 \mu\text{m}^2$ per pixel)
CCD Quantum efficiency	88% at 550 nm
CCD full well capacity	$\sim 120'000$ electrons/pixel
ADC levels	12 bit signal, 4096 levels: ~ 30 cts/digital level (low gain) ~ 5 cts/digital level (high gain)
Frame transfer time	≈ 2 ms
Time resolution	> 3 s
Typical integration times	10 s - 100 s
Wavelength range	Johnson V filter (centered at 550 nm)
Limit magnitude (10×100 s, 3σ) (50×100 s, 3σ) (200×100 s, 3σ)	17.6 (m_V) 18.2 (m_V) 19.0 (m_V)
Sensitivity to variations (10×100 s, 3σ)	$\Delta m_V < 0.1$, for $m_V < 16$

a. This parameter defines the factor by which the flux from any source within the UFOV (but outside the FOV) is reduced by multiple reflections before reaching the detector surface as background light

b. The unobstructed field of view (UFOV) defines the angle which has to be clear to space in order to avoid reflected light directly reaching the optics

II. Description of the instrument

1. Overall design

The OMC consists of an optical system focused onto a CCD detector. The optics are refractive with an entrance aperture of 5 cm diameter and a square field of view of $\approx 5^\circ \times 5^\circ$. A Johnson V filter allows photometric calibration in a standard system. An optical baffle ensures the necessary reduction of scattered sunlight and also the unwanted stray-light coming from non-solar sources outside the FOV. A deployable cover protected the optics from contamination during ground operations and early operations in orbit. It was released during the early steps of the commissioning phase. It now forms part of the baffle. See Figure 1 for a diagram of the OMC.

The camera unit is based on a large-format CCD (2055×1056 pixels) working in frame transfer mode (1024×1024 image area and 1024×1024 storage area, not exposed to light). This design, with a frame transfer time of around 2 ms, allows continuous measurements and makes it unnecessary to have a mechanical shutter. A LED light source within the optical cavity provides “flat-field” illumination of the CCD for on-board calibration.

2. The optics

The optical system, as shown in Figure 2, consists of:

- 1) a 6-fold lens system composed of two different types of radiation resistant glass
- 2) a filter assembly; the Johnson V filter has been defined with a combination of 2 different filters
- 3) a lens barrel giving mechanical support to the lenses and ensuring their alignment.

3. The CCD detector

The full well capacity is the maximum number of counts measurable per single pixel, in the present case $\approx 120,000$ cts. This parameter critically determines the dynamic range of the detector. The Analogue to Digital converters (ADCs) used in the OMC have the capability of digitising the analogue signal coming from the CCD read-out ports to 12 bits, i.e., they provide a discrete output in up to 4096 digital levels. The ADCs are designed to be operated with 2 gain values. At low gain, the full dynamic range of the CCD, 0 - 120,000 cts per pixel, is digitized into 0 - 4095 digital levels (DN), at a linear scale of ≈ 30 cts/DN. At high gain, only the 0 - 20,000 cts per pixel range is digitized into 0 - 4095 DN, with ≈ 5 cts/ DN. This allows a more accurate photometry in some cases down to approximately the noise limit of the CCD. Finally, the CCD is cooled by means of a passive radiator (illustrated in Fig. 1) to an operational temperature of around -80° C.

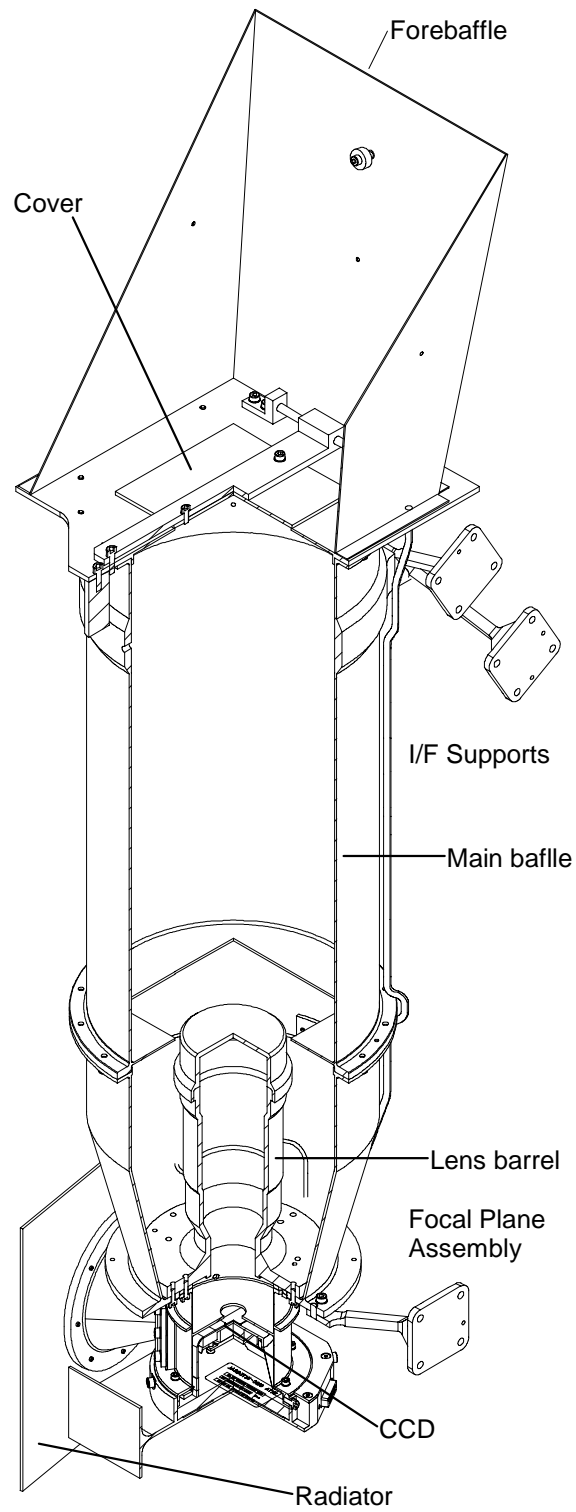


Figure 1. A 3-D cut of the OMC Camera Unit

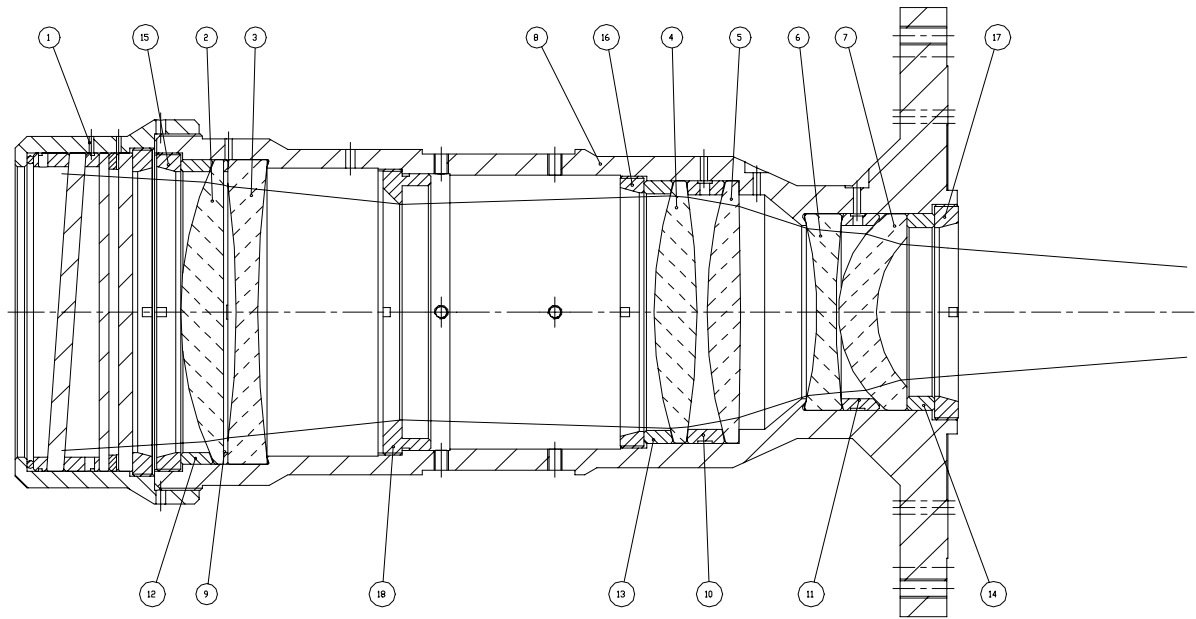


Figure 2. Optical system layout. 1: filter assembly housing; 2-7: lenses; 8: lens barrel; 9-14: spacers; 15-17: retainers; 18: aperture stop

III. Instrument operations

Because of telemetry constraints (only ≈ 2.2 kbps are allocated to the OMC) it is not possible to transmit the entire OMC image to the ground. For this reason windows are selected around the proposed gamma-ray target as well as other targets of interest in the same field of view. The observers obtain the data pertinent to their target, as well as all the other OMC CCD sub-windows taken during the observation (see also **Annexe on Integral Data Rights**). These additional targets are automatically selected from the OMC "Input Catalogue". Two observation modes are available to the observer: the normal and the fast monitoring modes.

1. Normal science operations mode

In the normal science operations mode, the OMC monitors the optical flux of a number of targets, including the high-energy sources within its FOV, other sources of interest, stars for photometric calibration and masked pixels from the CCD to monitor the dark current. Variable integration times during a pointing allow monitoring of both bright and faint sources. Operations are performed automatically in the following way:

- 1) The sequence starts by obtaining a series of images of ≈ 10 "astrometric" reference stars, spread over the field of view. This makes it possible to measure the pointing of the OMC optical axis with an accuracy of around 0.3 pixels ($\approx 6''$).
- 2) Then a set of photometric stars is observed (≈ 10 stars in the field of view with good photometric quality).
- 3) The CCD, centered in a target field, is then exposed during variable periods of time (10 - 100 s). After each exposure the full frame is transferred to the occulted part of the chip and the next integration starts. An optimum use of the CCD, from the point of view of the noise (read-out and cosmic rays) is obtained for integration times of around 100 s, so that for the faintest objects several exposures of 100 s are summed up during the analysis on ground. The number of integrations that can be added depends on the time during which the spacecraft keeps the same pointing without dithering (typically 30 min., i.e., around 18 individual measurements). Since the brightest stars saturate their corresponding pixels for such integration times, a combination of short and long exposures is performed so as to increase the magnitude range for a given field. The sequence of long and short integrations is defined automatically as a function of the targets to be monitored during each pointing. In this mode, variations with a time resolution down to around 2 minutes can be detected.
- 4) A number of windows (of typically 11×11 pixels, or $\approx 3' \times 3'$) are extracted around each object of interest and transmitted to the ground. When using the Proposal Generation Tool (PGT, see the **Integral Manual**) observers may specify a "Monitoring Window Size" for their target. The maximum allowed value is $30'$, corresponding to a $\approx 30' \times 30'$ square window. Any value smaller than $3'$ will, in fact, be executed with a $3' \times 3'$ window. Values

greater than $3' \times 3'$ are executed as a mosaic of smaller windows, e.g. several $3' \times 3'$ windows, piled side by side, which will have to be recombined on ground. Large window sizes can be useful for targets without precise, optically measured coordinates.

2. Fast monitoring mode

In the normal mode it is not possible to perform a continuous monitoring with a time resolution finer than 10 seconds. Therefore, when fast variability is expected, the fast monitoring mode should be chosen. With this mode, integration times in the range of 1 to 10 seconds are performed and only the sections of the CCD containing the target of interest are read from the CCD and transmitted. This of course implies that the position of the source is known with an accuracy better than the window size (11×11 pixels, i.e. $3' \times 3'$), and that the source is bright enough to be monitored with integration times below 10 s (see Fig. 6 below).

3. The OMC input catalogue

As explained above, besides the proposed target(s), the OMC observes astrometric and photometric stars and other targets of scientific interest within its field of view at a given time. For this purpose, a catalogue has been compiled by the OMC team containing over 500,000 sources, including:

- Known optical counterparts of gamma-ray sources
- Known optical counterparts of X-ray sources
- X-ray sources detected and catalogued by ROSAT
- Quasars observable with the OMC
- Additional known AGNs
- Known eruptive variable stars (including novae and cataclysmics)
- Variable objects which may require additional optical monitoring
- HIPPARCOS reference stars for positioning and photometrical calibration.

During the mission, additional sources of interest are added to the catalogue, namely:

- Newly discovered optical counterparts of high-energy sources, especially sources discovered during the Galactic Plane Survey.
- Regions of special interest for INTEGRAL science
- New supernovae
- New eruptive variable stars
- Any other Target of Opportunity (TOO).

For each scheduled observation the coordinates of all the targets of interest within the corresponding field of view are extracted from the OMC input catalogue. The table of targets of interest is included in the telecommands to be sent to the OMC before any new pointing, allowing the observer to identify all downloaded CCD windows.

4. Gamma-ray bursts and transient sources

The Integral Burst Alert System (IBAS) is located at the Integral Science Data Centre (ISDC) near Geneva. IBAS searches for gamma-ray bursts (GRB) using SPI/ACS triggers and IBIS/ISGRI detections and position measurements. If IBAS detects a GRB within the OMC FOV, a near-real-time command is sent to the OMC, via the Integral Mission Operations Centre (MOC), located in Darmstadt. Upon reception of this telecommand, the OMC stops the observations planned for this pointing and starts to monitor a single window of 81×81 pix ($\approx 24' \times 24'$) around the region where the burst has been detected, with a fixed integration time of 64 s. This “trigger” mode is active during the rest of the pointing, as well as during subsequent pointings as long as the bursting source is within the OMC FOV. The expected delay between the start of the burst and the start of OMC monitoring is less than 1 minute. Specifically, the OMC monitoring starts less than 15 seconds after the IBAS trigger. This makes it possible to obtain slightly delayed but simultaneous optical, X-ray and gamma-ray data of any burst taking place within the OMC FOV. Please note that at the time of writing of this document no GRB has yet occurred within the OMC FOV and that the delays mentioned above have been derived from tests performed after launch.

The **Annexe on Integral Science Data Rights** (section V.2) describes how and under which conditions the OMC data are distributed to the observers in the case of a gamma-ray burst or a transient.

IV. Instrument performances

1. Background and read-out noise

There are two main sources of background flux for the OMC, both related to the rather large angular pixel size of $17.5'' \times 17.5''$: scattered sunlight (zodiacal light) and unresolved stellar sources. Maximum background conditions correspond to pointings towards the galactic plane with maximum zodiacal light, while the minimum background are achieved around the galactic pole with minimum zodiacal light. Figure 3 shows the average number of stars brighter than a given magnitude contained within a single OMC pixel. It can be seen that, on average, no source confusion occurs for objects brighter than $m_V = 17$ at any galactic latitude. For $m_V = 18.0$ source confusion becomes problematic in regions very close to the galactic plane. It is important to stress that on the galactic plane there are in average more than one star per pixel with m_V between 17 and 19. The density of stars on the galactic plane indeed determines the limiting magnitude of the instrument. At galactic latitudes $|b| > 30^\circ$ the problem of source confusion becomes negligible, except for specific cases in which bright stars are separated by just a few arcseconds. The background measured in orbit corresponds well to the expected values.

The readout noise of the OMC as measured on ground is between 1-1.5 DNs/pixel (digital levels) for low gain and between 3-3.5 DNs/pixel in high gain, corresponding to 30-45 cts and 15-17 cts respectively. The readout noise measured in orbit is consistent with these values.

2. Limiting faint magnitude

Assuming a minimum level of background and the combination of 50 exposures of 100 s each, the limiting magnitude of the OMC is found to be $m_V = 18.2$ (3σ detection level). This value corresponds to a limiting sensitivity of the instrument of $4.5 \times 10^{-17} \text{ erg cm}^{-2} \text{ s}^{-1} \text{ \AA}^{-1}$ or, alternately, $1.25 \times 10^{-5} \text{ ph cm}^{-2} \text{ s}^{-1} \text{ \AA}^{-1}$, at 550 nm. At a maximum background level the limiting magnitude is $m_V = 17.8$. Note that these sensitivities can only be achieved for isolated stars for which the background can be properly estimated. Figure 4 shows the limiting magnitude for both maximum and minimum background as a function of integration time, assuming in all cases that 15 images have been combined to increase the signal to noise ratio. Figure 5 shows the limiting magnitude in best background conditions, and for different combinations of exposures.

Measurements in orbit show that the OMC is in average about 30% more sensitive than estimated during ground-based calibrations. However, the absolute photometric calibration changes with time and is continuously updated by the OMC team.

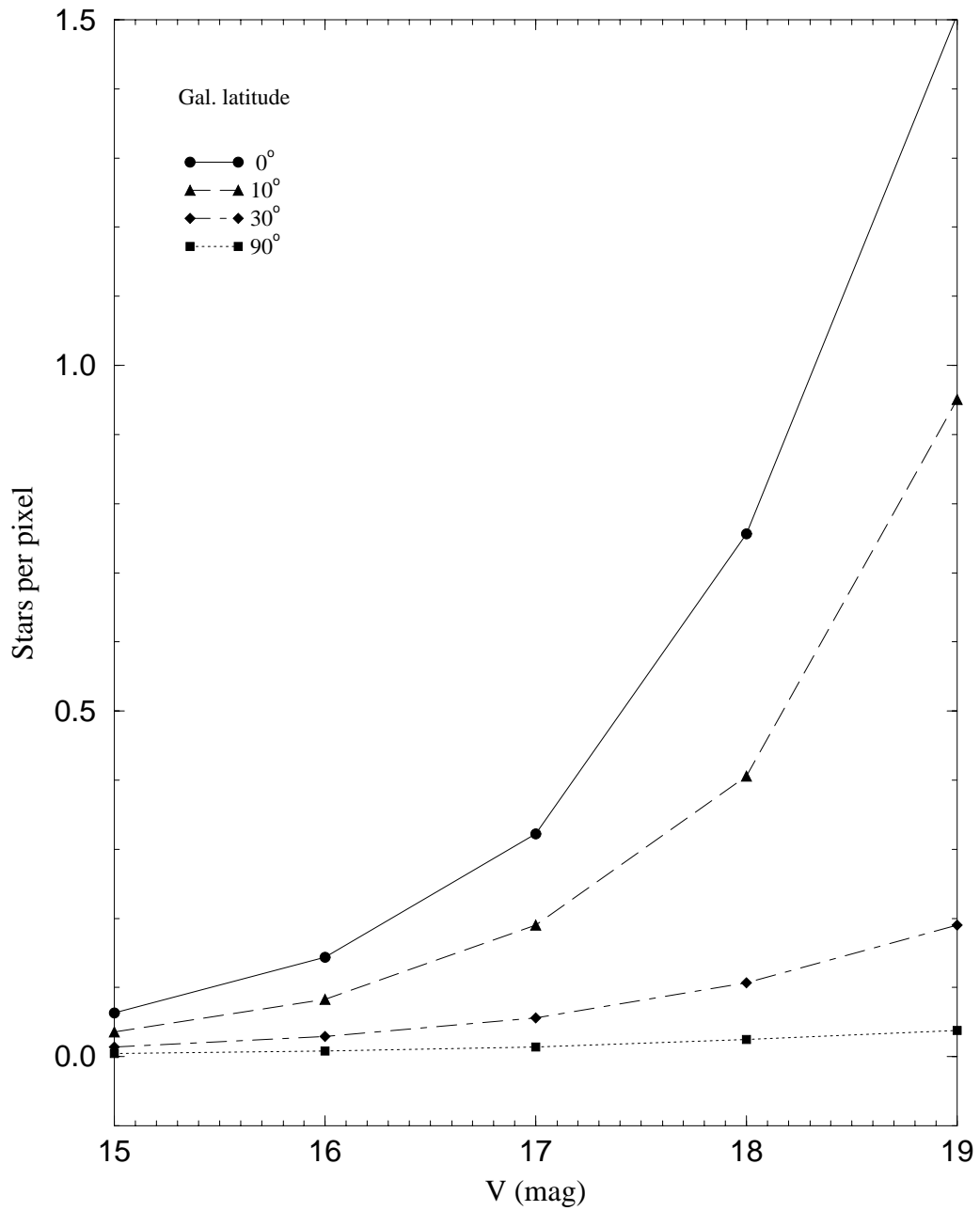


Figure 3. Average number of stars per pixel brighter than a given V magnitude at different galactic latitudes

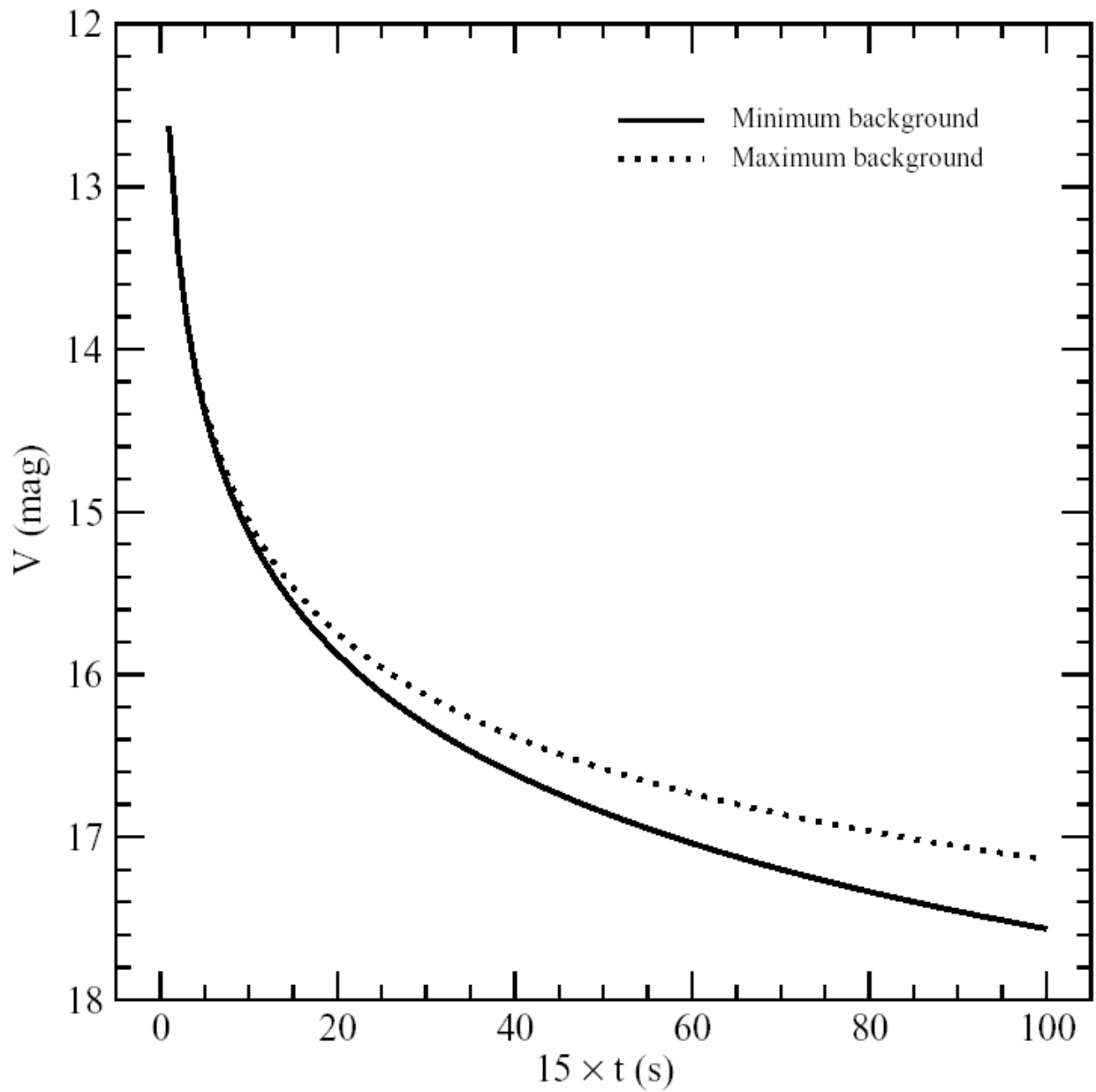


Figure 4. Limiting faint magnitude for a 3σ detection in the V band as a function of integration time. The best and the worst background cases are shown. It is assumed that 15 separate exposures, each with the integration time as given in the plot, have been combined together in order to increase the signal to noise ratio

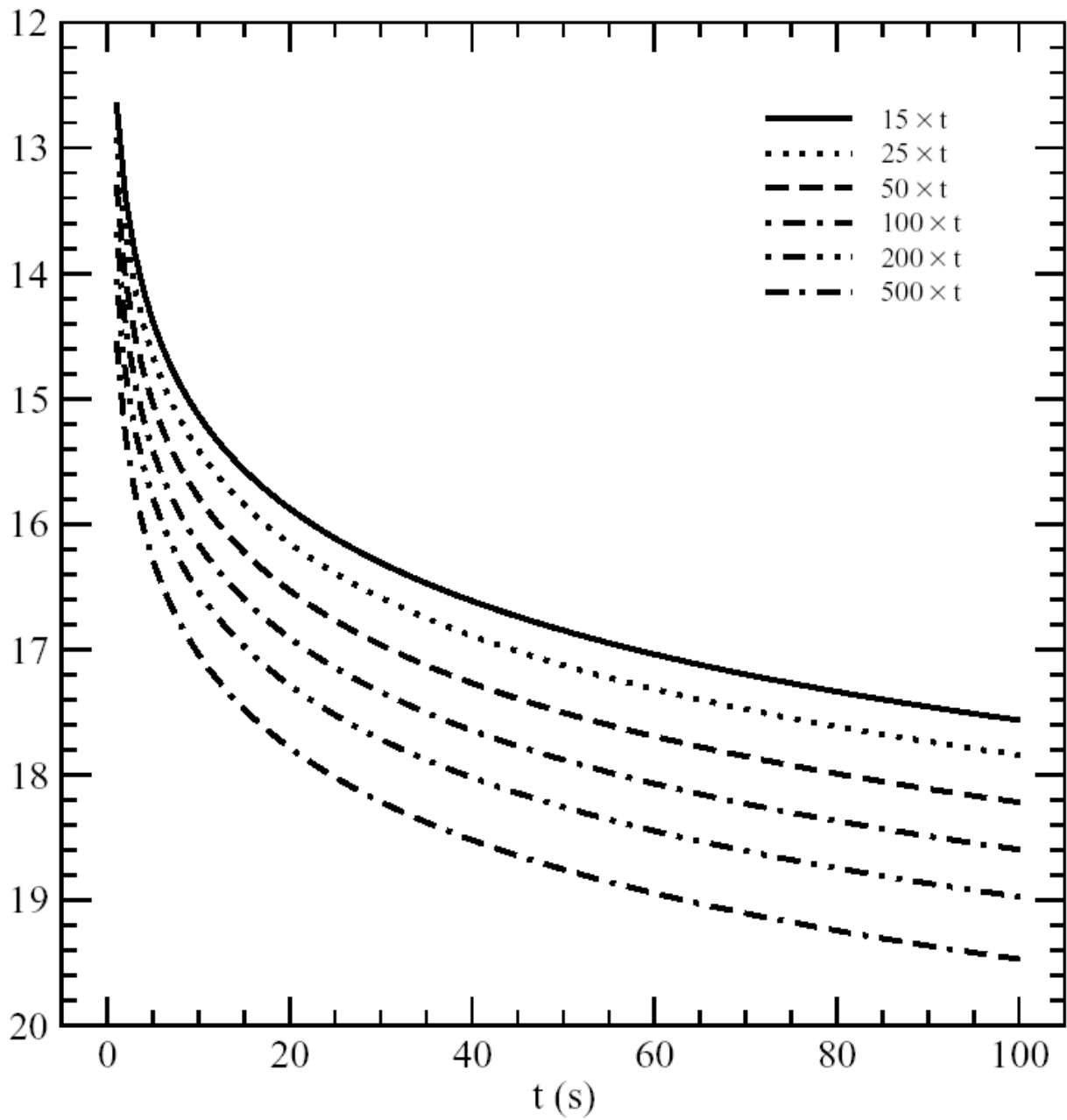


Figure 5. Limiting faint magnitude for a 3σ detection in the V band as a function of integration time. Best case background conditions are assumed (galactic pole, no zodiacal light). The curves correspond to different total numbers of images being combined

3. Limiting bright magnitude

The full well capacity of the CCD constrains the magnitude of the brightest stars that can be measured without pixel saturation for a given integration time. With 10 s integrations, the central pixel becomes saturated for objects brighter than $m_V=6$. With integrations of 100 s, even stars with $m_V\approx 9$ will start to saturate the CCD. Severe saturation of the CCD might imply losing the information from the surrounding pixels and potentially from the column containing the source, but no damage is expected on the detector. Figure 6 shows the predicted number of counts on the CCD as a function of V magnitude for a 10 s integration. This number corresponds to the counts expected in the central (brightest) pixel only. Finally, Figure 7 gives the integration time at which stars of different magnitudes will start to saturate the CCD.

4. Photometric accuracy

Table 2 shows the expected error (expressed in magnitudes) of a given measurement for the various "effective" integration times and magnitudes. "Effective" integration time means the total exposure after combining several shots. The value of 300 seconds corresponds to the "typical effective exposure" obtained by the OMC Standard Analysis at ISDC using the default parameters. A value around 900 seconds corresponds to the maximum effective exposure one can get in the OMC Standard Analysis (changing the default parameters). Of course, these values should be used only as a guide. The exact effective exposure depends on the source priority when downloading a given source and the sequence of on-board integrations (currently 100, 100, 30, 100, 10 seconds).

The values for photometric accuracy have been computed by taking into account the most current knowledge of the OMC instrument. One can see in Table 2 that good photometry can be performed in the V band for objects of quite different brightnesses. Note that these accuracies can only be obtained for isolated stars for which the background can be properly estimated. Furthermore, in case of dithering the photometric dispersion σ is > 0.015 (mag.) in all cases.

Table 2: Photometric accuracy for different background levels (in units of magnitude)

source $m_V \rightarrow$	8	10	12	14	16
effective^a exposures	assuming a typical background level:				
10 s	0.007	0.02	0.1	-	-
300 s	-	0.005	0.01	0.045	0.3
900 s	-	0.003	0.006	0.026	0.17

a. See text for the definition of an "effective" exposure

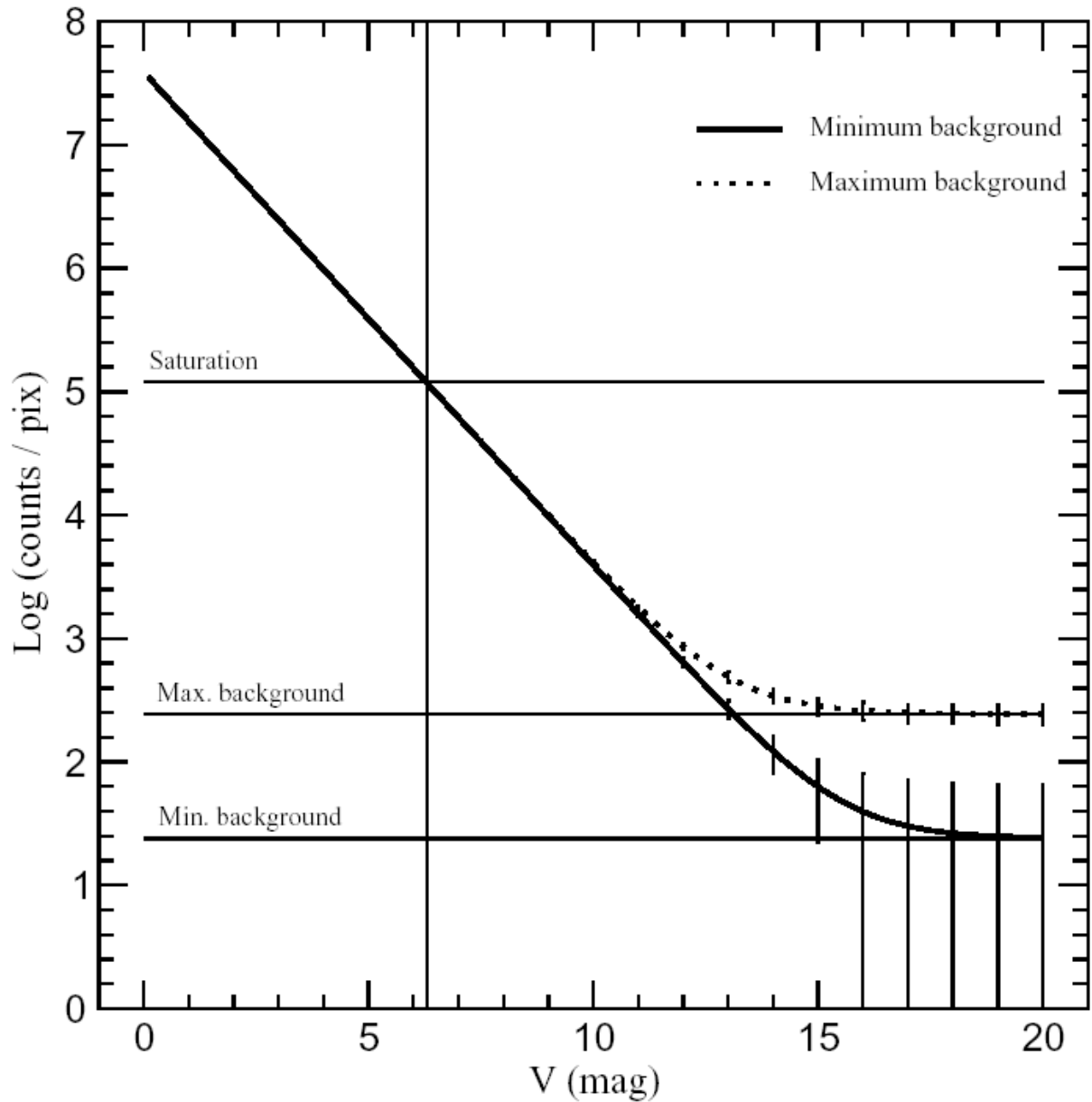


Figure 6. Expected number of counts on the central brightest pixel as a function of V magnitude, for an integration time of 10 s. The error bars correspond to 1σ . The plot also includes the expected background flux computed for maximum and minimum conditions

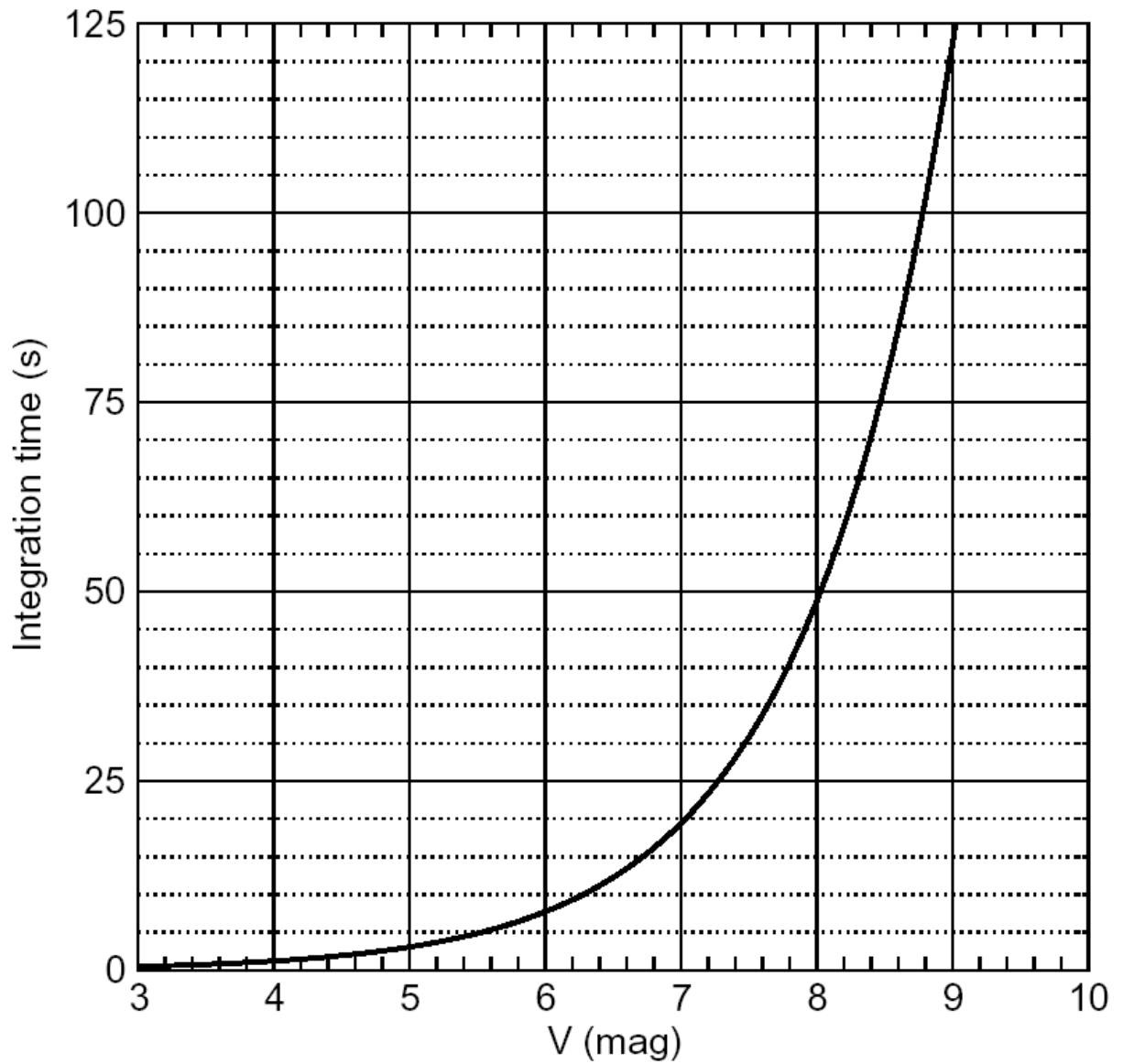


Figure 7. CCD saturation time as a function of V magnitude. Note that for integrations of 50 s, all stars brighter than $m_V=8$ will saturate the CCD. For the shortest OMC integration times, the brightest stars that can be observed should be fainter than $m_V\approx 3-4$

5. Focusing

The focusing capabilities of the OMC system have been verified to remain essentially unchanged over all the field of view, within the operational temperature range. The PSF precisely follows a Gaussian distribution with a FWHM ≈ 1.4 pixels, as shown in Figure 8.

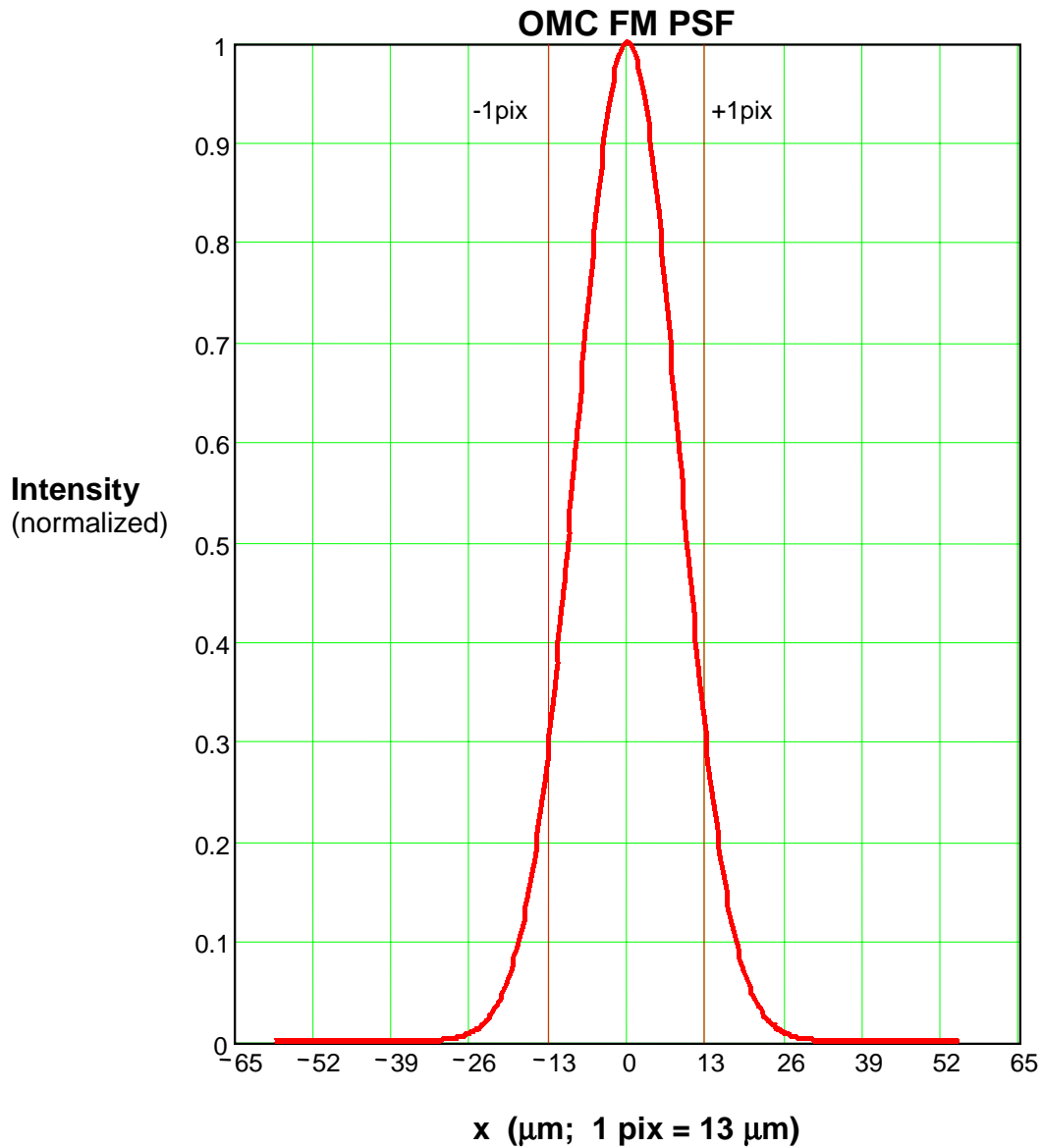


Figure 8. Point Spread Function of OMC (optical system + detector). The plot shows a fit to the average PSF measured under different conditions. The PSF measured in orbit follows a Gaussian with FWHM ≈ 1.4 pixels. More than 90% of the energy falls within a region of 3×3 pixels

V. Data products

Observers will receive the following data products per INTEGRAL pointing:

- The raw and corrected CCD sub-windows for all pre-defined sources in the field of view. The data are provided in a tabulated format with pixel values as vector entries in a column of the tables. CCD corrected windows will include flat-field calibration and dark current subtraction, but not the removal of cosmic rays.
- In addition, a series of tables with derived fluxes and magnitudes for all observed sources as a function of time. By default, photometrical analysis will be performed combining all images obtained within periods of around 10 minutes.

The ISDC provides a tool for extracting normal FITS images out of the tabulated pixel data, as part of the Off-line Scientific Analysis package (OSA).